




Three different structural lead(II) polymers constructed from newly designed chlorophenyl-imidazole dicarboxylate ligands

Zhi-Fang Yue, Zhen-Na Chen, Yuan-Hao Zhong & Gang Li

To cite this article: Zhi-Fang Yue, Zhen-Na Chen, Yuan-Hao Zhong & Gang Li (2015) Three different structural lead(II) polymers constructed from newly designed chlorophenyl-imidazole dicarboxylate ligands, Journal of Coordination Chemistry, 68:14, 2507-2519, DOI: 10.1080/00958972.2015.1051974

To link to this article: <http://dx.doi.org/10.1080/00958972.2015.1051974>

 View supplementary material 

 Accepted author version posted online: 20 May 2015.
Published online: 09 Jun 2015.

 Submit your article to this journal 

 Article views: 53

 View related articles 

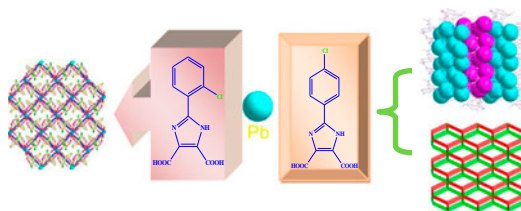
 View Crossmark data 

Three different structural lead(II) polymers constructed from newly designed chlorophenyl-imidazole dicarboxylate ligands

ZHI-FANG YUE, ZHEN-NA CHEN, YUAN-HAO ZHONG and GANG LI*

College of Chemistry and Molecular Engineering, Zhengzhou University, Zhengzhou, PR China

(Received 9 September 2014; accepted 18 March 2015)



Three different structural lead(II) polymers constructed from newly designed 2-chlorophenyl-imidazole dicarboxylate ligands.

A 1-D coordination polymer, $\{[\text{Pb}(o\text{-ClPhH}_2\text{IDC})_2] \cdot \text{H}_2\text{O}\}_n$ ($o\text{-ClPhH}_2\text{IDC}$ = 2-(2-chlorophenyl)-1H-imidazole-4,5-dicarboxylic acid) (1), a 2-D coordination polymer, $[\text{Pb}_3(p\text{-ClPhIDC})_2(\text{H}_2\text{O})]_n$ ($p\text{-ClPhH}_2\text{IDC}$ = 2-(4-chlorophenyl)-1H-imidazole-4,5-dicarboxylic acid) (2), and a 3-D polymer, $[\text{Pb}(p\text{-ClPhH}_2\text{IDC})_2]_n$ (3), have been obtained solvothermally and structurally characterized by elemental analyses, IR, and single-crystal X-ray diffraction. Although they were prepared with similar ligands and Pb^{2+} , polymers 1–3 show distinct structures. The X-ray powder diffraction and thermal properties of the polymers have been investigated. The influence of the reaction conditions to the final products and coordination of the organic ligands are discussed.

Keywords: Imidazole dicarboxylate; Lead; Polymer; Crystal structure; Property

1. Introduction

Along with rapid development of crystal engineering, researchers have obtained insight on preparation methods as well as potential applications of coordination polymers (CPs) [1–4]. Solvothermal synthesis is an important method because the final crystalline products of CPs can be altered by changing experimental reaction temperature, reaction time, solvent type, surfactant type, as well as metal centers, types of ligands, a ratios metal salts and ligands [5–8]. Although there have been efforts to explore the above factors, control of structures of CPs remains difficult. Factors governing the reaction and formation of solvothermal products are very complicated and more work on CPs needs to be done.

*Corresponding author. Email: gangli@zzu.edu.cn

Usually, the syntheses of CPs are focused on the incorporation of transition, rare-earth, and alkaline-earth metals as coordination centers. In contrast, relatively less attention has been paid to main group metals [9, 10]. Pb(II) as a heavy p-block metal ion provides opportunity to construct novel topologies and interesting properties owing to its large radius (covalent radius being 1.46 Å) [11–13], flexible stereochemical activity, and sensitive coordination environment. Compared with transition or lanthanide metals, few cases of Pb(II) CPs have been reported [14, 15].

We have investigated the substituent effect of a new imidazole dicarboxylate ligand, 2-(4-bromophenyl)-1*H*-imidazole-4,5-dicarboxylic acid (*p*-BrPhH₃IDC), with electron-withdrawing groups [16] and determined that *p*-BrPhH₃IDC shows strong coordination and various coordination modes. Since Cl is also electron withdrawing, it may have a similar substituent effect on a phenyl imidazole dicarboxylate ligand. Here, we introduce Cl to the phenyl unit getting two organic ligands, 2-(2-chlorophenyl)-1*H*-imidazole-4,5-dicarboxylic acid (*o*-ClPhH₃IDC) and 2-(4-chlorophenyl)-1*H*-imidazole-4,5-dicarboxylic acid (*p*-ClPhH₃IDC), and further probe their coordination. Three CPs, {[Pb(*o*-ClPhH₂IDC)₂·H₂O]_n} (1), [Pb₃(*p*-ClPhIDC)₂(H₂O)]_n (2) and [Pb(*p*-ClPhH₂IDC)₂]_n (3), have been solvothermally prepared. The structural features, thermal, and X-ray powder diffraction (XRPD) properties of the polymers are discussed.

2. Experimental

2.1. Materials and instrumentation

All chemicals were of reagent grade obtained from commercial sources and used without further purification. The ligands *o*-ClPhH₃IDC and *p*-ClPhH₃IDC were prepared according to the literature [17].

The C, H, and N microanalyses were carried out on a FLASH EA 1112 analyzer. IR spectra were recorded on a Nicolet NEXUS 470-FTIR spectrophotometer as KBr pellets from 400 to 4000 cm⁻¹. Thermogravimetric (TG) measurements were performed by heating the crystalline sample from 20 to 850 °C at a rate of 10 °C min⁻¹ in air on a Netzsch STA 409PC differential thermal analyzer. The XRPD was performed on a PANalytical X'Pert PRO diffractometer with monochromated Cu Kα radiation.

2.2. Preparation of {[Pb(*o*-ClPhH₂IDC)₂·H₂O]_n} (1)

A mixture of *o*-ClPhH₃IDC (13.3 mg, 0.05 mmol), Pb(NO₃)₂ (16.6 mg, 0.05 mmol), terephthalic acid (8.3 mg, 0.05 mmol), NaOH (0.008 g, 0.2 mmol), and EtOH/H₂O (3/4, 7 mL) was sealed in a 25 mL Teflon-lined autoclave and heated at 140 °C for 96 h. Then the reaction mixture was allowed to cool to room temperature at a rate of 10 °C h⁻¹. Colorless rod-like crystals of 1 were collected in 46% yield (based on Pb), washed with distilled water, and dried in air. Anal. Calcd for C₂₂H₁₄Cl₂N₄O₉Pb: C, 34.90; H, 1.85; N, 7.40%. Found: C, 35.01; H, 1.69; N, 7.37%. IR (cm⁻¹, KBr): 3442 (s), 3056 (w), 1518 (s), 1456 (m), 1405 (s), 1384 (m), 1356 (s), 1114 (w), 1097 (w), 1020 (w), 863 (w), 818 (m), 781 (w), 749 (m), 633 (w), 546 (w), 526 (w), 442 (w).

2.3. Preparation of $[Pb_3(p\text{-ClPhIDC})_2(H_2O)]_n$ (**2**)

A mixture of *p*-ClPhH₃IDC (26.6 mg, 0.1 mmol), Pb(OAc)₂·3H₂O (38.0 mg, 0.1 mmol), Et₃N (0.028 mL, 0.2 mmol), and EtOH/H₂O (3/4, 7 mL) was sealed in a 25 mL Teflon-lined autoclave and heated at 150 °C for 96 h. Then the reaction mixture was allowed to cool to room temperature at a rate of 10 °C h⁻¹. Colorless flake-shaped crystals of **2** were collected in 54% yield (based on *p*-ClPhH₃IDC), washed with distilled water, and dried in air. Anal. Calcd for C₂₂H₁₀Cl₂N₄O₉Pb₃: C, 22.63; H, 0.86; N, 4.80%. Found: C, 22.49; H, 1.08; N, 4.68%. IR (cm⁻¹, KBr): 3426 (m), 1547 (s), 1493 (s), 1421 (s), 1384 (s), 1335 (s), 1268 (m), 1253 (m), 1097 (s), 977 (w), 861 (w), 806 (s), 787 (m), 746 (m), 738 (m), 703 (w), 669 (w), 587 (w), 498 (w), 472 (w), 446 (w).

2.4. Preparation of $[Pb(p\text{-ClPhH}_2\text{IDC})_2]_n$ (**3**)

A mixture of *p*-ClPhH₃IDC (13.3 mg, 0.05 mmol), Pb(NO₃)₂ (16.6 mg, 0.05 mmol), terephthalic acid (8.3 mg, 0.05 mmol), NaOH (0.008 g, 0.2 mmol), and CH₃CN/H₂O (3/4, 7 mL) was sealed in a 25 mL Teflon-lined autoclave and heated at 140 °C for 96 h. Then the reaction mixture was allowed to cool to room temperature at a rate of 10 °C h⁻¹. Colorless cubic crystals of **3** were collected in 52% yield (based on Pb), washed with distilled water, and dried in air. Anal. Calcd for C₂₂H₁₀Cl₂N₄O₈Pb: C, 35.85; H, 1.36; N, 7.60%. Found: C, 35.59; H, 1.02; N, 7.45%. IR (cm⁻¹, KBr): 3425 (m), 3089 (m), 1676 (m), 1605 (s), 1557 (s), 1472 (s), 1371 (s), 1274 (m), 1114 (m), 1091 (s), 1014 (m), 966 (m), 844 (s), 783 (m), 737 (m), 701 (m), 665 (m), 629 (w), 574 (m), 522 (w), 464 (m), 422 (m).

2.5. Crystal structure determinations

Crystal measurements of **1–3** were obtained on a Bruker Smart APEXII CCD diffractometer with graphite-monochromated Mo K α radiation ($\lambda = 0.71073$ Å). All data were collected at room temperature using the ω -2 θ scan technique and corrected for Lorentz-polarization effects. Furthermore, a correction for secondary extinction was applied.

The three structures were solved by direct methods and expanded using the Fourier technique. The non-hydrogen atoms were refined with anisotropic thermal parameters. The hydrogens on C were positioned geometrically and refined using a riding model. The hydrogens on O were found at reasonable positions in the differential Fourier map. All hydrogens were included in the final refinement. All calculations were performed using the SHELXL-97 crystallographic software package [18, 19]. The final cycle of full-matrix least squares refinement was based on 5572 observed reflections and 361 variable parameters for **1**, 4059 observed reflections and 355 variable parameters for **2**, and 2153 observed reflections and 169 variable parameters for **3**. Crystal data and experimental details for **1–3** are contained in table 1. Selected bond lengths and angles, and hydrogen bond parameters of **1** and **3** are listed in tables 2 and 3, respectively.

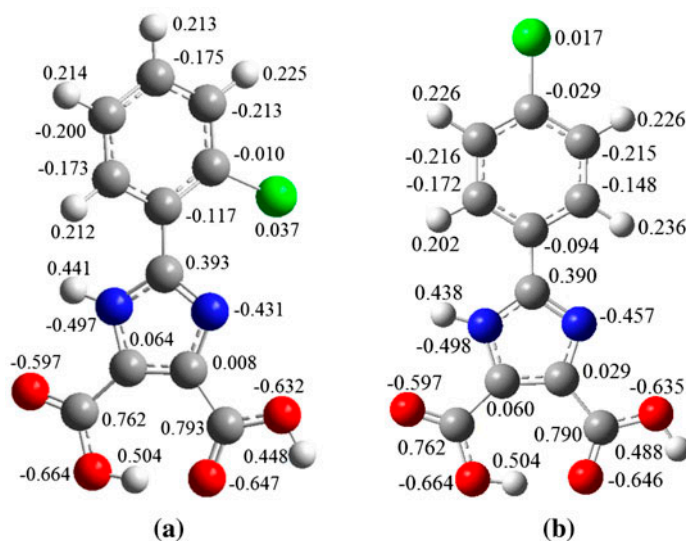
2.6. Quantum-chemical calculation

To analyze the coordination features of the two ligands (scheme 1), the geometries of *o*-ClPhH₃IDC and *p*-ClPhH₃IDC were fully optimized using density functional theory using Becke's three-parameter hybrid exchange functional and the Lee–Yang–Parr correlation

Table 1. Crystal data and structure refinement information for 1–3.

	1	2	3
Formula	C ₂₂ H ₁₄ Cl ₂ N ₄ O ₉ Pb	C ₂₂ H ₁₀ Cl ₂ N ₄ O ₉ Pb ₃	C ₂₂ H ₁₀ Cl ₂ N ₄ O ₈ Pb
F_w	756.46	1164.79	736.43
Crystal system	Monoclinic	Monoclinic	Tetragonal
Crystal size (mm)	0.23 × 0.21 × 0.14	0.27 × 0.24 × 0.18	0.27 × 0.25 × 0.24
Space group	$P2_1/n$	$P2_1/c$	$I4_1/a$
a (Å)	9.4958(8)	21.860(3)	17.1778(4)
b (Å)	13.4085(11)	8.2319(10)	17.1778(4)
c (Å)	19.4018(16)	13.3296(17)	15.9471(11)
α (°)	90	90	90
β (°)	99.3030(10)	92.629(2)	90
γ (°)	90	90	90
V (Å ³)	2437.8(4)	2396.2(5)	4705.6(4)
D_c (Mg m ⁻³)	2.061	3.229	2.079
Z	4	4	8
μ (mm ⁻¹)	7.201	21.315	7.456
Refns. collected/unique	14,580/5572	10,389/4059	4915/2153
	$R(\text{int}) = 0.0497$	$R(\text{int}) = 0.0598$	$R(\text{int}) = 0.0380$
Data/restraints/parameters	5572/2/361	4059/1128/355	2153/0/169
R	0.0387	0.0645	0.0294
R_w	0.0871	0.1790	0.0525
GOF on F^2	0.994	1.021	1.042
$\Delta\rho_{\text{max}}$ and $\Delta\rho_{\text{min}}$ (e Å ⁻³)	1.983 and -1.302	4.855 and -4.951	0.534 and -0.525

functional (B3LYP) [20–22] with the 6-31+G* basis set [23]. Harmonic vibrational frequencies were then determined at the same level to confirm that the optimized structures were local minima on the potential energy surfaces. The optimized geometries were used to carry



Scheme 1. The optimized geometries and NBO charge distributions of the free ligands *o*-CIPhH₃IDC (a) and *p*-CIPhH₃IDC (b). (The blue ball represents N, the red represents O, the gray represents C, and the white represents H [see <http://dx.doi.org/10.1080/00958972.2015.1051974> for color version]).

Table 2. Selected bond distances (Å) and angles (°) for 1–3.

1			
Pb(1)–N(3)	2.447(5)	Pb(1)–O(3)	2.457(4)
Pb(1)–O(6)	2.514(4)	Pb(1)–N(1)	2.601(5)
Pb(1)–O(8)#1	2.720(5)	N(3)–Pb(1)–O(3)	78.1(2)
N(3)–Pb(1)–O(6)	67.5(1)	O(3)–Pb(1)–O(6)	134.6(1)
N(3)–Pb(1)–N(1)	77.7(2)	O(3)–Pb(1)–N(1)	65.5(1)
O(6)–Pb(1)–N(1)	78.5(1)	N(3)–Pb(1)–O(8)#1	82.5(2)
O(3)–Pb(1)–O(8)#1	135.7(1)	O(6)–Pb(1)–O(8)#1	69.0(1)
N(1)–Pb(1)–O(8)#1	146.5(2)		
2			
Pb(1)–O(14)#1	2.365(4)	Pb(2)–O(30)	2.523(4)
Pb(1)–O(4)	2.550(4)	Pb(2)–N(2)#3	2.556(5)
Pb(1)–O(2)	2.652(4)	Pb(2)–N(4)#4	2.594(5)
Pb(1)–O(12)#2	2.679(4)	Pb(3)–O(13)	2.346(4)
Pb(1)–N(3)#1	2.701(5)	Pb(3)–O(9)	2.583(5)
Pb(2)–O(3)	2.262(5)	Pb(3)–O(5)	2.578(4)
Pb(2)–O(4)#3	2.456(4)	Pb(3)–O(2)	2.671(4)
O(14)#1–Pb(1)–O(4)	83.5(1)	O(3)–Pb(2)–N(2)#3	82.0(2)
O(14)#1–Pb(1)–O(2)	76.0(1)	O(4)#3–Pb(2)–N(2)#3	64.8(1)
O(4)–Pb(1)–O(2)	51.4(1)	O(30)–Pb(2)–N(2)#3	76.2(2)
O(14)#1–Pb(1)–O(12)#2	80.0(1)	O(3)–Pb(2)–N(4)#4	65.9(2)
O(4)–Pb(1)–O(12)#2	137.2(1)	O(4)#3–Pb(2)–N(4)#4	123.1(2)
O(2)–Pb(1)–O(12)#2	153.1(1)	O(30)–Pb(2)–N(4)#4	72.3(2)
O(14)#1–Pb(1)–N(3)#1	66.6(1)	N(2)#3–Pb(2)–N(4)#4	139.2(2)
O(4)–Pb(1)–N(3)#1	67.9(1)	O(13)–Pb(3)–O(9)	71.0(1)
O(2)–Pb(1)–N(3)#1	110.9(1)	O(13)–Pb(3)–O(5)	75.7(1)
O(12)#2–Pb(1)–N(3)#1	69.3(1)	O(9)–Pb(3)–O(5)	78.0(1)
O(3)–Pb(2)–O(4)#3	72.8(1)	O(13)–Pb(3)–O(2)	68.8(1)
O(3)–Pb(2)–O(30)	76.3(2)	O(9)–Pb(3)–O(2)	111.4(1)
O(4)#3–Pb(2)–O(30)	132.6(2)	O(5)–Pb(3)–O(2)	136.8(1)
3			
Pb(1)–O(3)	2.472(4)	Pb(1)–O(2)	2.637(4)
Pb(1)–N(2)	2.695(4)	N(2)#1–Pb(1)–N(2)	126.7(2)
O(3)–Pb(1)–O(3)#1	107.2(2)	O(2)–Pb(1)–N(2)#1	91.3(1)
O(3)–Pb(1)–O(2)#1	152.5(1)	O(3)–Pb(1)–N(2)	64.9(1)
O(3)–Pb(1)–O(2)	82.0(1)	O(2)#1–Pb(1)–O(2)	101.8(2)
O(3)–Pb(1)–N(2)#1	83.8(1)	O(2)–Pb(1)–N(2)	122.9(1)

Notes: Symmetry transformations used to generate equivalent atoms. For 1: #1: $-x + 3/2, y - 1/2, -z + 1/2$; #2: $-x + 3/2, y + 1/2, -z + 1/2$. For 2: #1: $x, -y + 3/2, z + 1/2$; #2: $-x, -y + 2, -z + 2$; #3: $-x, y + 1/2, -z + 3/2$; #4: $x, -y + 3/2, z - 1/2$; #5: $-x, y - 1/2, -z + 3/2$. For 3: #1: $-x + 2, -y + 1/2, z + 0$; #2: $y + 1/4, -x + 5/4, z + 1/4$; #3: $-y + 5/4, x - 1/4, z - 1/4$.

Table 3. Hydrogen bond distances (Å) and angles (°) for 1–3.

D–H...A	$d(\text{H...A})$	$d(\text{D...A})$	$\angle(\text{DHA})$
1			
O(7)–H(7)...O(5)	1.63	2.455(7)	177.8
O(1)–H(1)...O(4)	1.72	2.477(7)	153.4
O(9)–H(50)...O(6)#3	2.2(1)	3.021(7)	177(9)
O(9)–H(51)...O(2)#4	2.20(7)	2.852(8)	164(8)
N(2)–H(31)...O(9)#5	2.03(2)	2.863(7)	162(6)
N(4)–H(30)...O(9)#6	2.07(2)	2.918(7)	170(6)
3			
O(7)–H(7)...O(1)#3	1.67	2.474(5)	168.3

Notes: Symmetry transformations used to generate equivalent atoms: For 1: #3: $x - 1/2, -y + 1/2, z + 1/2$; #4: $x, y - 1, z + 1$; #5: $-x, -y + 1, -z + 1$; #6: $-x + 1, -y + 1, -z + 1$. For 3: #3: $-y + 5/4, x - 1/4, z - 1/4$.

out natural bond orbital (NBO) analyses [24] at the B3LYP/6-311++G** level of theory. All calculations were performed using the Gaussian 09 program.

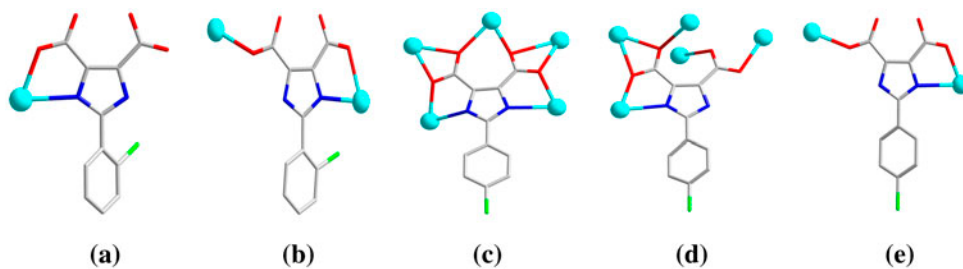
The computed results reveal that the negative NBO charges of *o*-ClPh₃IDC are -0.597 , -0.664 , -0.632 , and -0.647 for four carboxylate oxygens, -0.497 and -0.431 for two imidazole nitrogens, while in free *p*-ClPh₃IDC the negative NBO charges are -0.597 , -0.664 , -0.635 , and -0.646 for four carboxylate oxygens, -0.498 and -0.457 for two imidazole nitrogens (scheme 1). These values show that N and O may have strong coordination abilities under appropriate reaction conditions, on the other hand, the NBO charge distributions of oxygen and nitrogen for *o*-ClPh₃IDC and *p*-ClPh₃IDC are very close except one N. That is to say, the substituent effects of *o*-chlorophenyl and *p*-chlorophenyl groups are similar.

3. Results and discussion

3.1. Synthesis

From the crystal structures and solvothermal preparation, we determined that in **2** the imidazole-*H* and two COO-*H* are removed from *p*-ClPh₃IDC to form the triply deprotonated *p*-ClPhIDC³⁻. One COO-*H* is deprotonated in **1** and **3** leading to *o*-ClPh₂IDC⁻ or *p*-ClPh₂IDC⁻. The different deprotonation forms depend on pH values of the reaction solution. The pH of the reaction mixture of **2** is 8, which was adjusted using Et₃N. In contrast, the pH of the reaction mixture of **1** (or **3**) is 6, which was adjusted by NaOH. The higher pH value, thus, benefits the higher deprotonation. Compounds **1** and **3** have similar reaction temperature, molar ratio of reactants and pH value, however, the reaction solvents and ligands are different. The crystal structures of **1** and **3** are 1-D and 3-D, respectively. This indicates that the reaction medium is a very sensitive parameter for solvothermal preparation of CPs. The different deprotonation forms of *o*-ClPh₃IDC and *p*-ClPh₃IDC give different coordination modes (scheme 2), which further make different structures of **1**–**3**.

The anion of metal salt may affect the yield of final product. If Pb(OAc)₂ is changed to Pb(NO₃)₂ in the synthesis of **2**, only low yield of **2** could be generated, which suggests that NO₃⁻ plays an important role in formation of **2**. The similar case can be found in the syntheses of **1** and **3**. Compounds **1**–**3** have been obtained with medium yield by solvothermal reactions in EtOH–H₂O (3 : 4) or MeCN–H₂O (3 : 4) mixed solutions. Change in organic solvent or adoption of hydrothermal synthesis cannot result in any crystalline products of



Scheme 2. Coordination modes of the *o*-ClPh₃IDC and *p*-ClPh₃IDC ligands.

1–3, but some unidentified powders. The results indicate that the formation of the framework is influenced considerably by the nature of the solution. The selection of terephthalic acid in the synthesis of **1** and **3** is necessary. Without it, only powders were produced. We speculate that terephthalic acid may act as a “template” reagent to direct the extended structures of **1** and **3**.

Only several examples of Pb(II) CPs constructed by imidazole dicarboxylate ligand can be found [25–27]. The successful preparations of **1–3** provide CPs built by phenyl imidazole dicarboxylate ligands.

3.2. Crystal structure of crystalline polymer $\{[Pb(o-CIPhH_2IDC)_2] \cdot H_2O\}_n$ (**1**)

Crystal structure determination reveals that **1** crystallizes in the monoclinic $P2_1/n$ space group and features a 1-D infinite chain structure. The asymmetric unit contains one Pb(II), two *o*-CIPhH₂IDC[−] anions, and one free water. As shown in figure 1(a), the Pb(II) center is five coordinate showing a distorted trigonal-bipyramidal geometry. Pb(II) is surrounded by two five-membered chelating rings from *N,O*-bidentate *o*-CIPhH₂IDC[−] (N3–Pb1–O6, N1–Pb1–O3) and another carboxylate oxygen (O8#2) from the third *o*-CIPhH₂IDC[−] anion. The Pb–O and Pb–N distances are 2.447(5)–2.720(5) Å. The bond angles around Pb(II) vary from 65.5(1) to 146.5(2)°. The *o*-CIPhH₂IDC[−] ligands adopt two coordination modes, μ_1 -*kN,O* [scheme 2(a)] and μ_2 -*kN,O*: *kO'* [scheme 2(b)].

The bidentate *o*-CIPhH₂IDC[−] anions bridge adjacent Pb(II) cations to form an infinite chain. The intra-chain Pb··Pb distance is 9.4769(6) Å. The monodentate *o*-CIPhH₂IDC[−] anions are decorated on both sides of the 1-D chain [figure 1(b)]. As depicted in figure 1(c), along the *a*-axis adjacent chains are interlinked to produce a 3-D supramolecular framework through classical hydrogen bonding interactions between free water molecules (H(50)–O(9)–H(51)) and the carboxylate oxygen or imidazole nitrogen (O(9)–H(50)…O(6)#3, O(9)–H(51)…O(2)#4, N(2)–H(31)…O(9)#5 and N(4)–H(30)…O(9)#6). The charming 3-D motif with rhombic grid along the *c*-axis is illustrated in figure 1(d).

3.3. Crystal structure of crystalline polymer $[Pb_3(p-CIPhIDC)_2(H_2O)]_n$ (**2**)

X-ray determination shows that **2** crystallizes in the monoclinic $P2_1/c$ space group and features a sheet structure, in which there are three coordination environments around Pb(II). As shown in figure 2(a), the three Pb(II) ions have different coordination numbers. Pb1 is seven coordinate by six O and one N from three organic ligands. Pb2 is five coordinate by two five-membered rings (O3–N4#4 and O4#3–N2#3) and one oxygen (O30) of coordinated water. Pb3 is six coordinate with a distorted octahedral environment, in which the equatorial plane is occupied by four oxygens (O2, O13, O3, and O5) from two *p*-CIPhIDC^{3−} ligands with two monodentate oxygens (O9, O5#2) at the apical sites (see Supporting Information, figure S1 [see online supplemental material at <http://dx.doi.org/10.1080/00958972.2015.1051974>]). Bond distances of Pb–O and Pb–N are 2.262(5)–2.679(4) Å and 2.556(5)–2.701(4) Å, respectively. The bond angles around Pb(II) vary from 51.4(1) to 153.1(1)°. The *p*-CIPhIDC^{3−} ligands adopt two kinds of uncommon coordination modes, μ_5 -*kN,O*: *kO,O'*: *kO',O''*: *kO'',O'''*: *kO''',N'* [scheme 2(c)] and μ_5 -*kN,O*: *kO,O'*: *kO'*: *kO''*: *kO'''* [scheme 2(d)].

As shown in figure 2(b), the layer structure of **2** contains complicated waving chains along the *b*-axis, which are composed of left- and right-handed helical chains. This 2-D layer has a thickness of six center metal Pb(II) ions. Neighboring infinite chains are

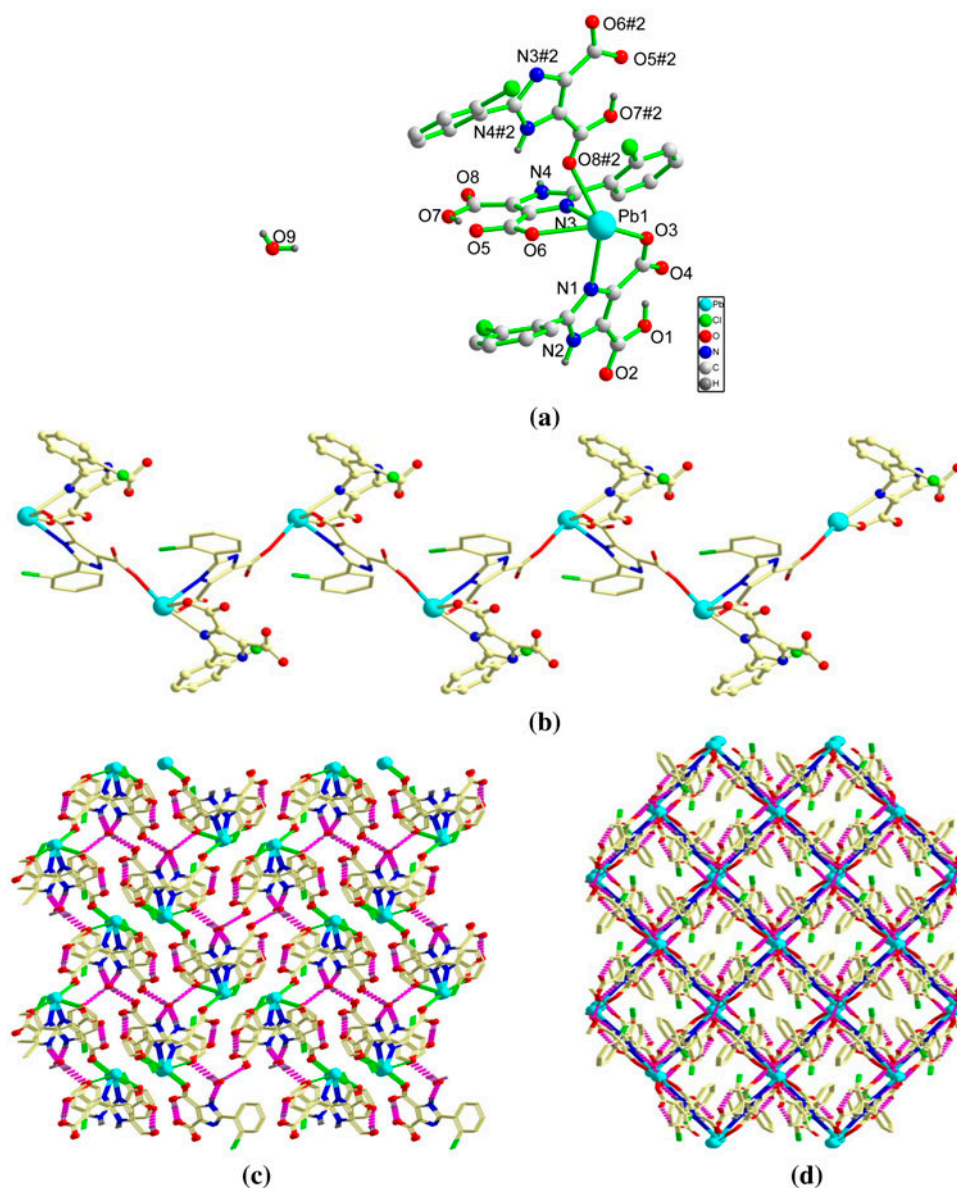


Figure 1. (a) Coordination environment of Pb(II) in **1** (some hydrogens are omitted for clarity), (b) the 1-D infinite serrated chain in **1**, (c) 3-D supramolecular framework of **1** along the *a*-axis showing intermolecular H-bonds between the chains, and (d) the 3-D motif with rhombic grid along the *c*-axis of **1**.

interpenetrated to each other and stack in a ...ABAB... fashion to develop an intricate 2-D framework along the *a*-axis as shown in figure 2(c).

3.4. Crystal structures of crystalline polymer $[Pb(p\text{-ClPhH}_2\text{IDC})_2]_n$ (**3**)

X-ray single-crystal diffraction reveals that **3** crystallizes in the tetragonal $I4_1/a$ space group. As depicted in figure S3, the coordination environment around Pb(II) is best described as a

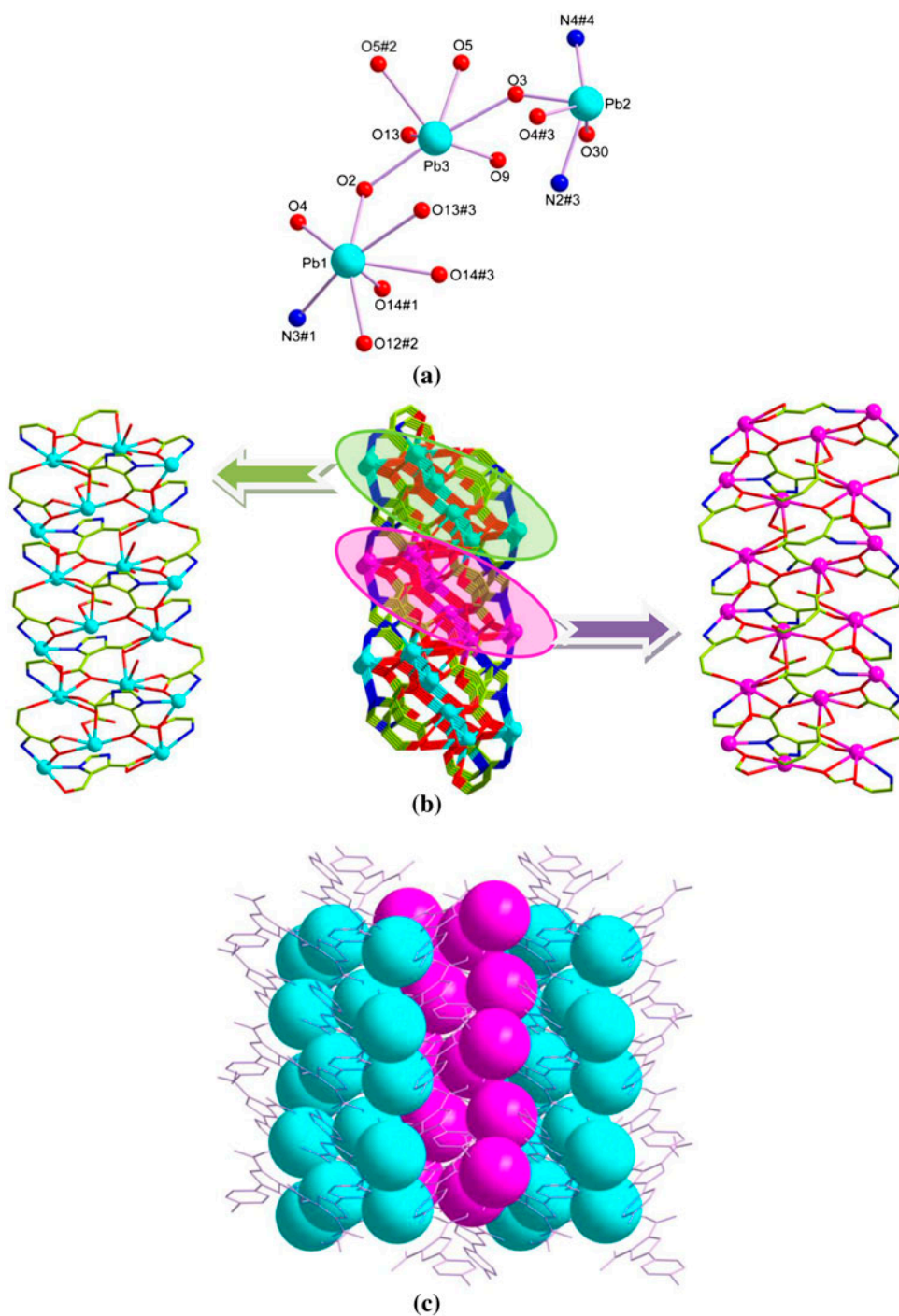


Figure 2. (a) Coordination environments of Pb(II) ions in **2** (some atoms are omitted for clarity), (b) the waving chains along the *b*-axis composed of left- and right-handed helical chains (some atoms are omitted for clarity), and (c) the layer of **2** composed of *p*-ClPhIDC³⁻ and Pb(II) along the *a*-axis.

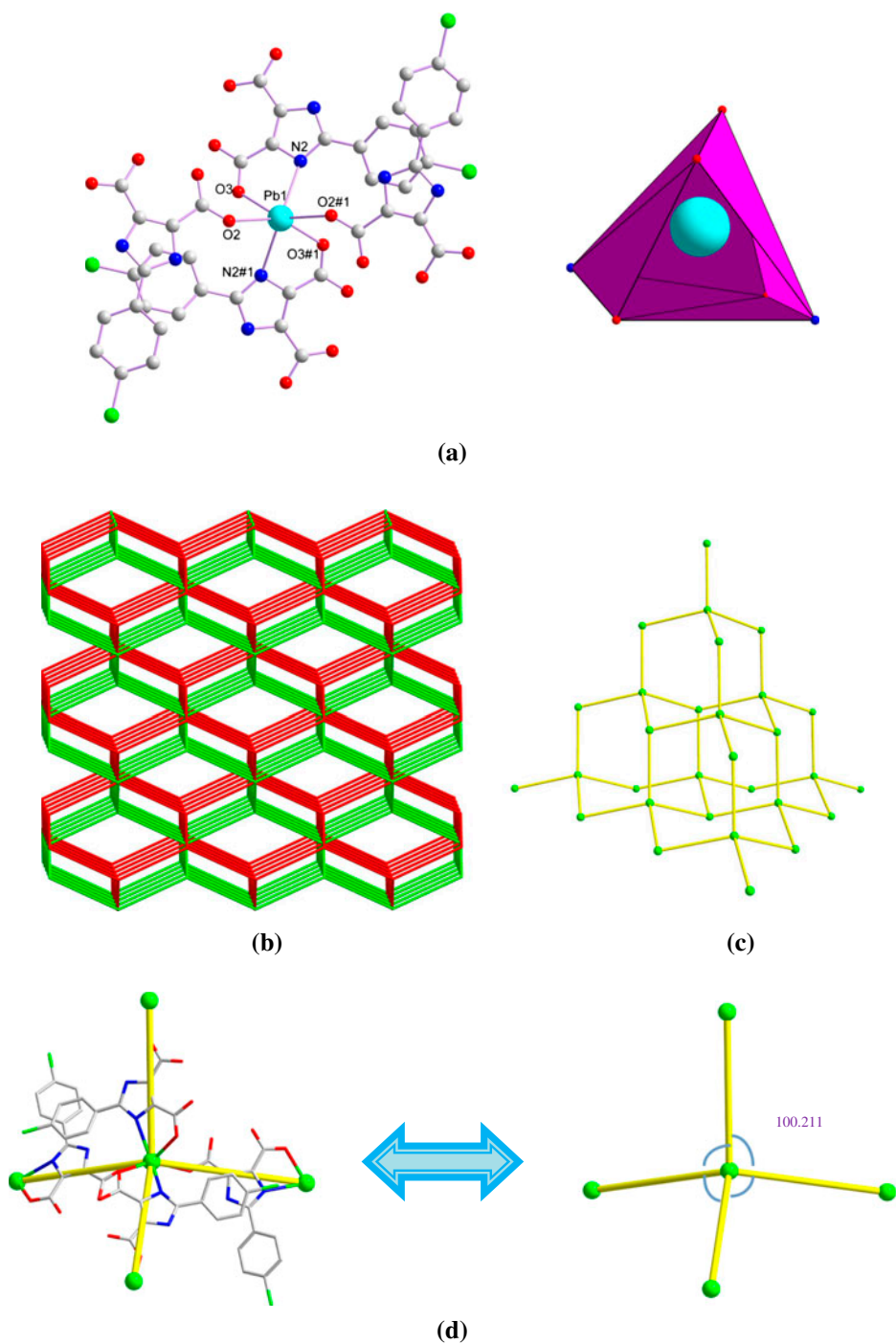


Figure 3. (a) Coordination environment of Pb(II) in **3** (hydrogens are omitted for clarity), (b) the 3-D 2-fold interpenetrating network for **3**, (c) the diamond cubic crystal structure of **3**, and (d) the tetrahedral building block in **3**.

distorted $[\text{PbN}_2\text{O}_4]$ octahedral environment by four oxygens (O2, O3, O2#1, O3#1) and two nitrogens (N2, N2#1) from four $p\text{-ClPhH}_2\text{IDC}^-$ anions. The Pb–O distances are 2.472 (4) and 2.637(4) Å, respectively. The Pb–N distance is 2.695(4) Å. The bond angles around Pb(II) vary from 64.9(1) to 152.5(1)°. Each imidazole dicarboxylate adopts a $\mu_2\text{-kN}_2\text{O}$: $k\text{O}'$ mode [scheme 2(e)] connecting two Pb(II) ions.

The topological consideration of **3** is obtained using OLEX. Each $p\text{-ClPhH}_2\text{IDC}^-$ can be regarded as a linear two-connected linker. Each Pb ion is surrounded by four $p\text{-ClPhH}_2\text{IDC}^-$ anions, which can be represented by a 4-connected unit. Thus, the 3-D framework of **3** can be described as a uninodal 4-connected 2-fold topology with the Schläfli symbol of $(6^5\cdot 8)$ [figure 3(b)] and the Pb(II) is coordinated by four bridging ligands forming the network similar with the diamond cubic crystal structure [figure 3(c)]. The distance of adjacent $\text{Pb}\cdots\text{Pb}$ is 9.469 Å and the four angles as tagged in figure 3(d) are 100.211(0)°, while the other two angles are 130.201(0)°.

3.5. Infrared spectra, thermal analyses, and XRPD

IR spectra of the polymers display characteristic absorption bands for water molecules, carboxylate, imidazole, and phenyl units. The strong and broad absorptions at 3400–3650 cm^{-1} indicate the presence of $\nu_{\text{N-H}}$ and the $\nu_{\text{O-H}}$ stretching frequencies of imidazole and water. The $\nu_{\text{as}}(\text{COO}^-)$ and $\nu_{\text{s}}(\text{COO}^-)$ vibrations can be observed at 1533–1566 cm^{-1} and 1443–1488 cm^{-1} , respectively. The characteristic IR band for phenyl at 840–860 cm^{-1} due to $\delta_{\text{C-H}}$ vibrations can be found at 863 cm^{-1} for **1**, 861 cm^{-1} for **2**, and 844 cm^{-1} for **3**.

To characterize the thermal stability of **1–3**, thermogravimetric analyses were studied in air (figure 4). For **1**, the first weight loss of 2.05% (Calcd 2.38%) from 74 to 105 °C can be assigned to loss of solvent water. The second weight loss of 68.93% between 105 and 340 °C is consistent with loss of corresponding organic units of $o\text{-ClPhH}_2\text{IDC}^-$

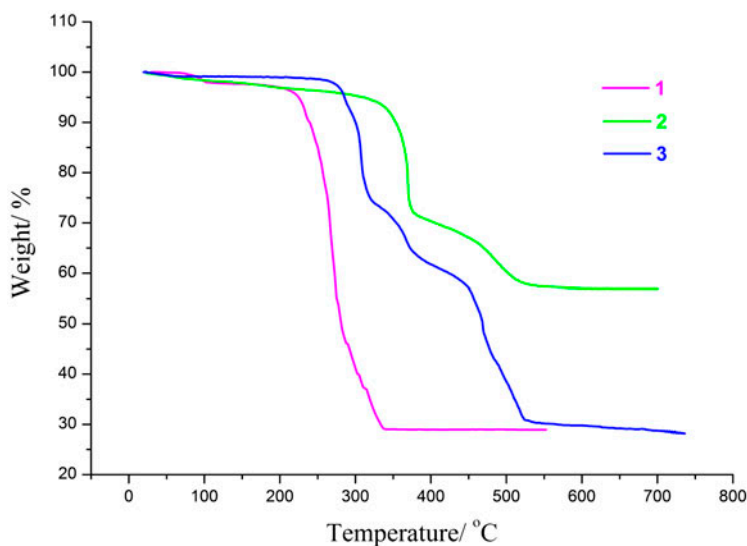


Figure 4. TG analysis profiles of **1–3**.

(Calcd 70.20%). The remaining weight of 29.02% (Calcd 29.51%) is observed from 340 to 557 °C, corresponding to the final product PbO.

For **2**, an initial weight loss from 133 to 430 °C arises from the loss of one coordinated water molecule, two chlorophenyl units, and two $\mu\text{-COO}^-$ units (obsd. 28.25%; Calcd 27.96%). Further weight loss from 430 to 580 °C corresponds to decomposition of the remaining $p\text{-ClPhIDC}^{3-}$ (obsd. 11.47%; Calcd 9.53%). Finally, a plateau region is observed from 580 to 700 °C, indicating the final residue of 3PbO (obsd. 57.08%; Calcd 57.49%).

Polymer **3** reveals a weight loss of 39.72% (Calcd 42.23%) from 247 to 436 °C corresponding to release of two chlorophenyl units and two $\mu\text{-COO}^-$ units, and then, the remaining organic units of $p\text{-ClPhH}_2\text{IDC}^-$ decompose from 436 to 585 °C (obsd. 29.11%, Calcd 30.15%). Finally, a plateau region is observed from 585 to 736 °C. The weight of remaining residue is 29.77% corresponding to PbO (Calcd 30.31%).

The XRPD was used to confirm the phase purity of the polymers, and most peak positions of simulated and experimental patterns are in agreement with each other. The dissimilarities in intensity may be due to the preferred orientation of the crystalline powder samples (Supporting Information, figures S2–S4).

Photoluminescent properties of the three polymers and free $o\text{-ClPhH}_3\text{IDC}$ and $p\text{-ClPhH}_3\text{IDC}$ were recorded at room temperature under the same experimental conditions. Unfortunately, **1–3** show very weak luminescence, almost no emission, attributed to the quenching effect of the Pb(II) cation or chloride [25].

4. Conclusion

Three distinct structural Pb(II) polymers, **1–3**, have been solvothermally constructed and characterized by single-crystal X-ray diffraction. The results demonstrate that the flexible $o\text{-ClPhH}_3\text{IDC}$ and $p\text{-ClPhH}_3\text{IDC}$ ligands can fine-tune their configuration to meet the geometric requirement of the metal atoms and have the potential for synthesizing new CPs. Further studies based on the organic ligands will be reported in due course.

Supplementary material

CCDC nos. 1003845, 938761, and 938759 contain the supplementary crystallographic data for **1–3**, respectively. The data can be obtained free of charge from the Cambridge Crystallographic Data Centre via www.ccdc.cam.ac.uk/data_request/cif.

Disclosure statement

No potential conflict of interest was reported by the authors.

Funding

This work was supported by National Natural Science Foundation of China [grant number 21341002], [grant number J1210060]; Program for New Century Excellent Talents in University [grant number NCET-10-0139]; the Natural Science Foundation of Henan Education Department [grant number 13A150655].

References

- [1] M. Du, C.-P. Li, C.-S. Liu, S.-M. Fang. *Coord. Chem. Rev.*, **257**, 1282 (2013).
- [2] Y. Chen, S.-Q. Ma. *Inorg. Chem.*, **32**, 81 (2012).
- [3] M.-Y. Masoomi, A. Morsali. *Coord. Chem. Rev.*, **256**, 2921 (2012).
- [4] H.-L. Jiang, Q. Xu. *Chem. Commun.*, **47**, 3351 (2011).
- [5] M.-X. Liang, C.-Z. Ruan, D. Sun, X.-J. Kong, Y.-P. Ren, L.-S. Long, R.-B. Huang, L.-S. Zheng. *Inorg. Chem.*, **53**, 897 (2014).
- [6] Z.-C. Zhang, Y.-F. Chen, X.-B. Xu, J.-C. Zhang, G.-L. Xiang, W. He, X. Wang. *Angew. Chem., Int. Ed.*, **53**, 429 (2014).
- [7] K. Liu, X. Han, Y.-C. Zou, Y. Peng, G.-H. Li, Z. Shi, S.-H. Feng. *Inorg. Chem. Commun.*, **39**, 131 (2014).
- [8] O.-K. Farha, J.-T. Hupp. *Acc. Chem. Res.*, **43**, 1166 (2010).
- [9] J.-D. Lin, S.-T. Wu, Z.-H. Li, S.-W. Du. *CrystEngComm.*, **12**, 4252 (2010).
- [10] X.-X. Xu, Y. Lu, E.-B. Wang, Y. Ma, X.-L. Bai. *Cryst. Growth Des.*, **6**, 2029 (2006).
- [11] P. Farina, T. Latter, W. Levason, G. Reid. *Dalton Trans.*, **42**, 4714 (2013).
- [12] B. Cordero, V. Gómez, A.-E. Platero-Prats, M. Revés, J. Echeverría, E. Cremades, F. Barragán, S. Alvarez. *Dalton Trans.*, **37**, 2832 (2008).
- [13] A.-M. Najar, I.-S. Tidmarsh, M.-D. Ward. *CrystEngComm.*, **12**, 3642 (2010).
- [14] L.-N. Li, S.-Q. Zhang, L. Han, Z.-H. Sun, J.-H. Luo, M.-H. Hong. *Cryst. Growth Des.*, **13**, 106 (2013).
- [15] C. Gabriel, M. Perikli, C.-P. Raptopoulou, A. Terzis, V. Psycharis, C. Mateescu, T. Jakusch, T. Kiss, M. Bertmer, A. Salifoglou. *Inorg. Chem.*, **51**, 9282 (2012).
- [16] Y. Zhang, B.-B. Guo, L. Li, S.-F. Liu, G. Li. *Cryst. Growth Des.*, **13**, 367 (2013).
- [17] A.-V. Lebedev, A.-B. Lebedeva, V.-D. Sheludiyakov, E.-A. Kovaleva, O.-L. Ustinova, V.-V. Shatunov. *Russ. J. Gen. Chem.*, **77**, 949 (2007).
- [18] G.-M. Sheldrick. *SHELX-97, Program for the Solution and Refinement of Crystal Structures*, University of Göttingen, Germany (1997).
- [19] G.-M. Sheldrick. *Acta Crystallogr., Sect. A: Found. Crystallogr.*, **64**, 112 (2008).
- [20] A.-D. Becke. *J. Chem. Phys.*, **98**, 5648 (1993).
- [21] C. Lee, W. Yang, R.-G. Parr. *Phys. Rev. B*, **37**, 785 (1988).
- [22] P.-J. Stephens, F.-J. Devlin, C.-F. Chabalowski, M.-J. Frisch. *J. Phys. Chem.*, **98**, 11623 (1994).
- [23] W.-J. Hehre, L. Radom, P.-R. Schleyer, J.-A. Pople. *Ab initio Molecular Orbital Theory*, John Wiley & Sons, New York (1987).
- [24] E.-D. Glendening, A.-E. Reed, J.-E. Carpenter, F. Weinhold. *NBO (Version 3.1)*, Theoretical Chemistry Institute, University of Wisconsin, Madison, WI (2001).
- [25] W.-Y. Wang, Z.-L. Yang, C.-J. Wang, H.-J. Lu, S.-Q. Zang, G. Li. *CrystEngComm.*, **13**, 4895 (2011).
- [26] Z.-F. Xiong, Y.-L. Li, C.-J. Wang, G. Li. *Dalton Trans.*, **42**, 4885 (2013).
- [27] Y. Zhang, P.-F. Yuan, Y.-Y. Zhu, G. Li. *Dalton Trans.*, **42**, 14776 (2013).